Biodegradation, ecotoxicity and UV254/H2O2 treatment of imidazole, 1-methyl-imidazole and N,N'-alkyl-imidazolium chlorides in water

Elsevier Editorial System(tm) for Water Research

Manuscript Draft

Manuscript Number:

Title: Biodegradation, ecotoxicity and UV254/H2O2 treatment of imidazole, 1-methyl-imidazole and N,N'-alkyl-imidazolium chlorides in water

Article Type: Research Paper

Keywords: ionic liquids, imidazole, biodegradation, ecotoxicity, H2O2 photolysis, kinetic modeling

Corresponding Author: Mr. Danilo Spasiano, PhD

Corresponding Author's Institution: Politecnico di Bari

First Author: Danilo Spasiano, PhD

Order of Authors: Danilo Spasiano, PhD; Antonietta Siciliano; Marco Race; Raffaele Marotta; Marco Guida; Roberto Andreozzi; Francesco Pirozzi

Abstract: Imidazole-based compounds are used as reagents for the manufacturing of other compounds including imidazolium-based ionic liquids, which have been recently proposed as a green alternative to conventional solvents. Since some imidazole-based compounds have been demonstrated to be harmful to aquatic organisms, the removal of imidazole, 1-methylimidazole, 1-ethyl-3-methyl-imidazolium chloride and 1-butyl-3-methyl-imidazolium chloride from aqueous solutions was attempted by biological oxidation, direct UV254 photolysis, and UV254/H2O2 process at pH 5.5 and 8.5. Results showed that UV254/H2O2 treatment is an effective tool for the removal of the selected compounds at both pHs. In fact, the kinetic constants of the reaction between the photogenerated HO radicals and the four target compounds, estimated by means of both numerical and competition kinetic method, range between 2.32*10^9 M-1*s-1 and 5.52 *10^9 M-1*s-1. Moreover, an ecotoxicity assessment of the contaminated water before and after initial treatment without further processing was assessed by using two living aquatic organisms: Raphidocelis subcapitata and Daphnia magna. The results of this assessment not only corresponded closely to previous findings (in terms of EC50 values) reported in the literature, but also indicated that, in some cases, UV254/H2O2 oxidation by-products could be even more toxic than parent compounds.

Suggested Reviewers: Sixto Malato PhD
Director, Plataforma Solar de Almerìa, Spain.
sixto.malato@psa.es

Gianluca Li Puma PhD
Ordinary Professor, Environmental Nanocatalysis & Photoreaction Engineering Department of Chemical E, Loughborough University
G.Lipuma@lboro.ac.uk

Sara Castiglioni PhD

Head of the Environmental BIomarkers Unit, Department of Environmental Health Sciences, Mario Negri Institute for Pharmacological Research
sara.castiglioni@marionegri.it

Vittorio Loddo PhD
Associate Professor, Dip. di Ingegneria Chimica dei Processi e dei Materiali, Università degli studi di Palermo
Vittorio.loddo@unipa.it

Santiago Esplugas PhD
Ordinary Professor, Chemical Engineering Dept., University of Barcelona
santi.esplugas@ub.edu

To Editor of
Water Research

Dear Editor,

please find enclosed a copy of the original manuscript: "Biodegradation, ecotoxicity and UV_{254}/H_2O_2 treatment of imidazole, 1-methyl-imidazole and N,N'-alkyl- imidazolium chlorides in water" by D. Spasiano, A. Siciliano, M. Race, R. Marotta, M. Guida, R. Andreozzi, F. Pirozzi, which we submit to Water Research. We believe that the findings of the proposed manuscript are relevant to the scope of Water Research and will be of interest to its readership.

Since their industrial use is increasing, imidazole-containing compounds and, in particular, imidazolium-based ionic liquids were recently added to the class of new emerging xenobiotics described as "Contaminant on Horizon". At the best of our knowledge, this is the first investigation regarding the degradation of imidazole, 1-methylimidazole, 1-ethyl-3-methyl-imidazolium chloride and 1-butyl-3-methyl-imidazolium chloride from aqueous solutions using the UV_{254}/H_2O_2 advanced oxidative process. Moreover, for the first time the kinetic constants for HO radical attack on 1-ethyl-3-methyl-imidazolium chloride and 1-butyl-3-methyl-imidazolium chloride were estimated. Finally, ecotoxicity assessments were carried out not only on the contaminated solutions, but also on the effluents at different treatment times.

The proposed manuscript has not been published or presented elsewhere in part or in entirety, and is not under consideration by another Journal. All the Authors have approved the proposal and agree with submission of the manuscript to Water Research. There are no conflicts of interest to declare.

Moreover,

• Six keywords and four highlights are provided in the text;

• Highlights and References are in the correct format;

Thank you for your consideration. We look forward to hearing from you.

Sincerely

The Authors

Highlights

- UV/H_2O_2 process was used to remove imidazole-based compounds in aqueous solutions
- The kinetic constants for HO attack on imidazole and its derivatives were estimated
- The ecotoxicity evolution was monitored during the chemical process
- An ecotoxicity increase was observed during the treatment of alkylimidazolium salts

Graphical Abstract

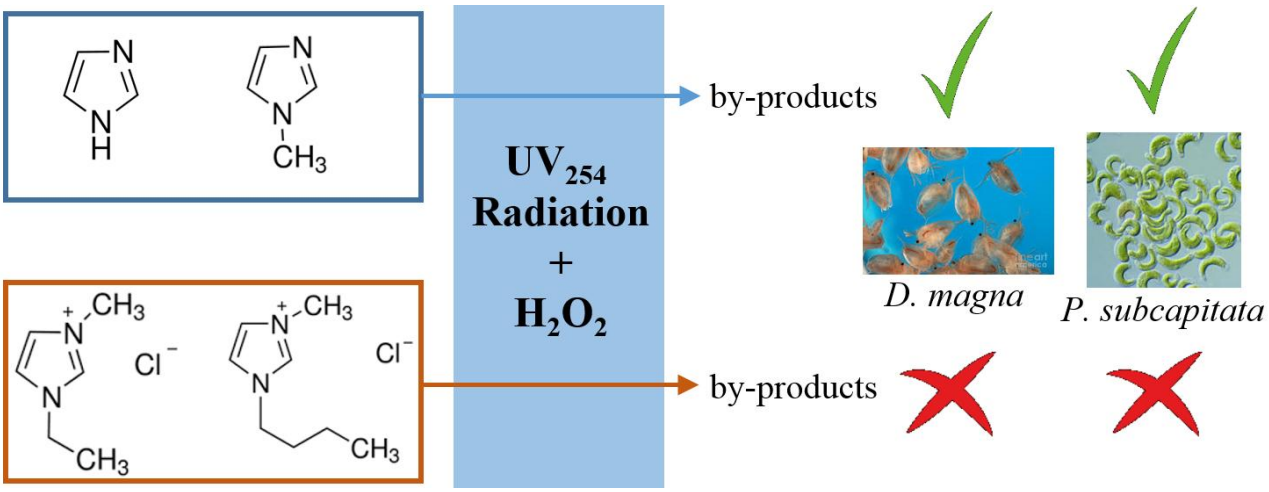

Biodegradation, ecotoxicity and UV_{254}/H_2O_2 treatment of imidazole, 1-methyl-imidazole and N,N'-alkyl-imidazolium chlorides in water

D. Spasiano[1a], A. Siciliano[b], M. Race[c], R. Marotta[2d], M. Guida[b], R. Andreozzi[d], F. Pirozzi[c]

[a] Dipartimento di Ingegneria Civile, Ambientale, del Territorio, Edile e di Chimica, Politecnico di Bari, Via E. Orabona, 4 – 70126 – Bari, Italia.

[b] Dipartimento di Biologia, Università di Napoli Federico II, Via Cinthia – 80126 – Napoli, Italia.

[c] Dipartimento di Ingegneria Civile, Edile ed Ambientale, Università di Napoli Federico II, Via Claudio, 21 – 80125 – Napoli, Italia.

[d] Dipartimento di Ingegneria Chimica, dei Materiali e della Produzione Industriale, Università di Napoli Federico II, p.le V. Tecchio, 80 – 80125 – Napoli, Italia.

[1] first corresponding Author: tel.: (+39) 0805963240; danilo.spasiano@poliba.it (D. Spasiano).

[2] second corresponding Author: tel.: (+39) 0817682968; rmarotta@unina.it (R. Marotta).

Keywords: ionic liquids, imidazole, biodegradation, ecotoxicity, H_2O_2 photolysis, kinetic modeling.

Abstract

Imidazole-based compounds are used as reagents for the manufacturing of other compounds including imidazolium-based ionic liquids, which have been recently proposed as a green alternative to conventional solvents. Since some imidazole-based compounds have been demonstrated to be harmful to aquatic organisms, the removal of imidazole, 1-methylimidazole, 1-ethyl-3-methyl-imidazolium chloride and 1-butyl-3-methyl-imidazolium chloride from aqueous solutions was attempted by biological oxidation, direct UV_{254} photolysis, and UV_{254}/H_2O_2 process at pH 5.5 and 8.5. Results showed that UV_{254}/H_2O_2 treatment is an effective tool for the removal of

the selected compounds at both pHs. In fact, the kinetic constants of the reaction between the photogenerated HO radicals and the four target compounds, estimated by means of both numerical and competition kinetic method, range between $2.32 \cdot 10^9$ $M^{-1} \cdot s^{-1}$ and $5.52 \cdot 10^9$ $M^{-1} \cdot s^{-1}$. Moreover, an ecotoxicity assessment of the contaminated water before and after initial treatment without further processing was assessed by using two living aquatic organisms: *Raphidocelis subcapitata* and *Daphnia magna*. The results of this assessment not only corresponded closely to previous findings (in terms of EC_{50} values) reported in the literature, but also indicated that, in some cases, UV_{254}/H_2O_2 oxidation by-products could be even more toxic than parent compounds.

1. Introduction

Numerous imidazole-containing compounds have received in the past considerable attention because of their availability and wide range of practical applications. For example, different molecules containing an imidazolinic ring in their structure, such as metronidazole, nitrosoimidazole, megazol, clonidine, guanfacine, and lofexidine hydrochloride exhibit pharmacological and biological activities (Kumar, 2010). Imidazole and its methyl-derivatives are extensively used as corrosion inhibitors of iron and copper (Zhang et al., 2009). Moreover, 1-methylimidazole is used for manufacturing of pharmaceuticals, pesticides, ion-exchange resins, dyeing auxiliaries, photographic chemicals, polyurethanes, curing agent for epoxy resins and ionic liquids (*Ullmann's Encyclopedia of Industrial Chemistry*).

Imidazolium-based ionic liquids (IMI-ILs) due to their low vapor pressure and flammability and high solvent proprieties for organic molecules, are frequently used in a wide range of biological applications and for the preparation of surfactants, plasticizers, antimicrobial and anti-inflammatory agents, scaffolds for biomimetic applications and membranes for oxygen transport (Dupont and Suarez, 2006; Anderson and Long, 2010). They are viewed as potential alternatives to conventional industrial solvents due to their marked chemical and thermal inertness, and could be used as

catalysts for many reactions. Therefore, it is likely that IMI-ILs will continue to be manufactured and used on an industrial scale in future.

This fact raises several concerns about their environmental impact, particularly since IMI-ILs are poorly or negligibly biodegradable (Jordan and Gathergood, 2015; Stolte et al., 2008; Romero et al., 2008; Garcia et al., 2005). It has been demonstrated that imidazolium-based ILs exhibit moderate to high toxicity towards aquatic organisms. In some cases this can be of the same order as traditional organic solvents but can reach two to four orders of magnitude higher. (Bubalo et al., 2014; Cho et al., 2008; Bernot et al., 2005). This clearly may raise questions about their "green" character.

Toxicity of IMI-ILs has previously been investigated using both aquatic and non-aquatic organisms to assess their ability to induce cellular and sub-cellular damage (e.g. viability, inhibition of the activity of specific enzymes, genotoxicity) (Peric et al., 2014; Biczak et al., 2014; Wu et al., 2013). Until now, the results have generally indicated that the effect of ionic liquids on biological systems increases with increasing lipophilicity and, in particular, lengthening alkyl chains (Pham et al., 2008; Jastorff et al., 2005; Matzke et al., 2007). I IMI-ILs with longer alkyl chains are more lipophilic than those with shorter ones and are able to pass through cell membranes. Additionally, imidazole and pyridine-based ILs generally display higher toxicity than aliphatic chain-based ILs (Petkovic et al, 2011). It has also been shown that the anionic form had little influence on the toxicity of ILs (Matzke et al., 2008).

Although to date there are no studies that demonstrate the presence of ILs as pollutants in sewage, industrial or civil treatment plant effluents, or in surface waters, their presence in water bodies cannot be totally ruled out now or in future. It is worthy to observe that Richardson et al. (Richardson and Ternes, 2014) recently added these compounds to the class of new emerging xenobiotics described as "Contaminant on Horizon". Since the industrial use of ILs is increasing, many risk scenarios exist for IMI-ILs as contaminants in industrial effluents. Thus, the risk of damage to the aquatic environment deserves consideration and means for decontamination should be assessed.

77 Advanced Oxidation Processes (AOPs) are based on the production of very high reactive oxidant
78 species, such as hydroxyl radicals (Rosenfeldt et al., 2006; Haag and Yao, 1992) and may provide
79 feasible solutions for the removal of non-biodegradable IMI-ILs from wastewater. Recent studies
80 demonstrated the possibility of reaching a complete removal of selected imidazolium-based species
81 at ambient conditions through the adoption of Fenton (Fe^{2+}/H_2O_2) and Fenton-like (Fe^{3+}/H_2O_2)
82 processes (Bocos et al., 2016; Munoz et al., 2015; Domínguez et al., 2014; Siedlecka et al., 2009;
83 Siedlecka et al., 2008). Unfortunately, high H_2O_2 doses are required and iron precipitates are
84 formed, reducing the oxidation activity. Furthermore, some investigations focused on the use of
85 ultraviolet photolysis of hydrogen peroxide (UV_{254}/H_2O_2) for oxidation of alkyl-imidazolium-based
86 ILs in water (Czerwicka et al., 2009; Stepnowski and Zaleska, 2005). These demonstrated that the
87 removal efficiency was affected by the length of the n-alkyl chain substituted at position 1 of the 1-
88 alkyl-3-methyl-imidazolium ring. The main oxidation intermediates and by-products formed during
89 the UV_{254}/H_2O_2 process were also identified. Currently, a lack of information remains about the
90 kinetic constant values of the reactions between these substances and the photogenerated HO
91 radicals, which are necessary for a UV_{254}/H_2O_2 treatment-unit design, and little is known about the
92 ecotoxicity of the by-products that could arise from this treatment.
93 Consequently, the aims of the present investigation are: i) to evaluate the biodegradability and
94 UV_{254} photolysis of imidazole (Imid), 1-methyl-imidazole (1MI) and some water soluble 1-alkyl-3-
95 methyl-imidazolium chlorides (1E3MI and 1B3MI) (Figure 1); ii) to estimate the kinetic constants
96 of the reaction between the target compounds and HO radicals formed by UV_{254}/H_2O_2 system; iii)
97 to evalute the ecotoxicity of the contaminated solutions before and after exposure to the UV_{254}/H_2O_2
98 process. For this purpose, two freshwater living organisms, algae *Raphidocelis Subcapitata* and
99 water flea *Daphnia Magna*, were used as bio-indicators for toxicity.
100 The investigation on the acute toxicities of the selected imidazolium based compounds and their by-
101 products is relevant to future discussions regarding the chronic toxicities, treatment, control and fate
102 of these substances and their derivatives in the environment.

2. Materials and methods

2.1. Materials

Hydrogen peroxide (30% v/v), Imid (≥99% w/w), 1MI (99% v/v), 1E3MI (98% w/w), 1B3MI (≥ 98.0% w/w), acetonitrile (≥99.9% v/v), ammonium acetate (≥98% w/w), ammonium chloride (99.99% w/w), calcium chloride (>99.9% w/w), benzoic acid (≥99.5% w/w), boric acid (>99.5% w/w), catalase from *Micrococcus lysodeikticus* (200191 $U \cdot ml^{-1}$), cobalt(II) chloride hexahydrate (97% w/w), copper(II) chloride dehydrate (99.99% w/w), hydrochloric acid (37% v/v), iron(III) chloride (97% w/w), magnesium sulfate heptahydrate (≥98% w/w), manganese(II) chloride (≥99% w/w), magnesium chloride hexahydrate (>99.9% w/w), mercury(II) chloride (99% w/w), potassium chloride (99% w/w), potassium dichromate (≥99% w/w), potassium phosphate dibasic (>98% w/w) and monobasic (99% w/w), sodium bicarbonate (≥99% w/w), sodium chloride (>99.9% w/w), sodium dihydrogen phosphate dodecahydrate (≥99% w/w), sodium hydroxide (≥98% w/w), sodium molybdate dihydrate (≥99% w/w), sodium nitrate (≥99% w/w), disodium ethylenediamine-tetraacetate dihydrate (≥99% w/w), zinc chloride (≥98% w/w), and sulfuric acid were purchased from Sigma-Aldrich. All the solution were prepared using bi-distilled water.

Activated sludge, taken from a Wastewater Treatment Plant at Nola (Naples, Italy), was used as our biomass to be spiked with the selected imidazole-containing compounds to study their biodegradability.

2.2. Analytical methods

Concentrations of hydrogen peroxide, Imid, 1MI, 1E3MI, 1B3MI, and benzoic acid (BA) were evaluated through HPLC analysis. Specifically, an HPLC (1100 Agilent) apparatus was equipped with a Synergy 4u Polar-RP 80A. A mobile phase, flowing at 1.0 ml min^{-1}, of acetonitrile (A) and a buffer solution (B) of 20.0 mM of ammonium acetate dissolved in water for HPLC was used. A linear gradient was adopted starting with 10% A to 30% A, from the 10^{th} to the 30^{th} minute of each analysis, with a subsequent re-equilibrium time of 4 min.

Total organic carbon (TOC) and chemical oxygen demand (COD) were monitored by a TOC analyzer (Shimadzu 5000 A) and Hack® cuvette test respectively. Measurements at 620 nm were carried out with a UV–vis spectrophotometer (Agilent).

The pH of the solutions was measured and tracked with an Orion 420A+ pH-meter (Thermo).

D. magna viability and mobility were observed with a stereomicroscope (LEICA EZ4-HD) and visualized on a computer. *R. subcapitata* density was determined by an indirect procedure using a spectrophotometer (Hach Lange DR5000) and a 5 cm cuvette.

2.3. Experimental apparatus and procedures

2.3.1. Biodegradability assessment apparatus and procedures

The composition of the inorganic medium used for the biodegradability test was carried out in accordance with Urano and Kato (Urano and Kato, 1986). Five ml of a mixture of K_2HPO_4 ($25.75 \cdot 10^{-3}$ mg·l^{-1}), KH_2PO_4 ($8.5 \cdot 10^{-3}$ mg·l^{-1}), $Na_2HPO_4 \cdot 12H_2O$ ($44.6 \cdot 10^{-3}$ mg·l^{-1}) and NH_4Cl ($1.7 \cdot 10^{-3}$ mg·l^{-1}), 0.5 ml of an aqueous solution of $MgSO_4 \cdot 7H_2O$ ($22.5 \cdot 10^{-3}$ mg·l^{-1}), 0.5 ml of $CaCl_2$ ($27.5 \cdot 10^{-3}$ mg·l^{-1}) and 1 ml of $FeCl_3 \cdot 6H_2O$ ($0.25 \cdot 10^{-3}$ mg·l^{-1}) were added to the bio-reactor. The biodegradation tests were conducted as previously described (Andreozzi et al., 2006) and each sample solution was prepared in a 250 ml reactor with fixed concentration of dry matter. For this purpose, the activated sludge was diluted with the bi-distilled water to a concentration of 3.0 g·l^{-1}. The tests were carried out at constant temperature (25° C), the sample solutions were stirred, aerated (by air bubbling), and the pH was regulated at 7.0 with HCl or NaOH.

Abiotic control tests (using $HgCl_2$ to inactivate the sludge) were performed in order to check an eventual adsorption of the tested compounds. The samples were taken at fixed times and filtered through regenerated Merck Millipore cellulose filters (0.45 μm) before analysis.

The total suspended solids (TSS) and volatile suspended solids (VSS) of the activated sludge were evaluated according to the standard procedures (APHA, AWWA, WEF, 2005).

154 The substrate concentration was monitored until complete degradation or up to 28 days. When
155 necessary, in order to acclimate the biomass, the recharges with mineral medium and substrate
156 were made until reaching the initial volume and recovering the starting conditions (substrate
157 concentration equal to 10 mg·l-1).
158 The biodegradation investigations were performed in triplicate and in batch conditions for each
159 tested compound.
160

161 **2.3.2. Cylindrical batch photoreactor and procedures**

162 In order to evaluate the kinetics of Imid, 1MI, 1E3MI, and 1B3MI oxidation with the UV_{254}/H_2O_2
163 process, a traditional cylindrical batch photoreactor was used as shown in Figure 2. The
164 contaminated solutions were exposed to the radiation emitted by a low-pressure mercury lamp (17
165 W) mainly emitting at 254 nm (Helios Italquartz) in the 0.480 l (V) batch photoreactor with a path
166 length (*z*) equal to 2.20 cm. The reactor, thermostated at 25 °C, was covered with aluminum foil.
167 The reactor had two inlets for supplying reactants and for withdrawing samples. The photon flux
168 emitted by the UV lamp at 254 nm (I_0), equal to $2.86 \cdot 10^{-6}$ ein·s^{-1}, was estimated through hydrogen
169 peroxide actinometry (Goldstein et al., 2007).
170 The reacting solutions were prepared by adding one of the target compounds (Imid, 1MI, 1E3MI
171 and 1B3MI) and H_2O_2 to bi-distilled water. The initial concentration of the target compounds used
172 in the experimental runs was equal to almost 10 mg·l^{-1}, for the experimental runs for kinetic
173 modeling, and 150 mg·l^{-1}, for the experimental runs to assess the eco-toxicity of the UV_{254}/H_2O_2
174 process by-products. The initial imidazolium based compounds concentrations were chosen in order
175 to simplify the analytical procedures for monitoring substrate consumption. For those experimental
176 runs devoted to the comparison kinetics method, BA was added to the reacting solution as reference
177 compound (Buxton et al., 1988; Onstein et al., 1999).

178 To evaluate the effect of pH on the process kinetics, the reacting solution pH was adjusted to 5.5 or
179 8.5 by the addition of NaOH and H_2SO_4 diluted solutions. All the experimental runs estimating
180 kinetic parameters were carried out in triplicate.
181
182 **2.3.3. Eco-toxicity assessment apparatus and procedures**
183 For toxicity assessment, $K_2Cr_2O_7$ was used as the toxicity reference. The following salts were used
184 for the preparation of artificial freshwater: $CaCl_2 \cdot 2H_2O$, $MgSO_4 \cdot 7H_2O$, KCl, $NaHCO_3$, $NaNO_3$,
185 NH_4Cl, $MgCl_2 \cdot 6H_2O$, K_2HPO_4, KH_2PO_4, $FeCl_3 \cdot 6H_2O$, $Na_2EDTA \cdot 2H_2O$, H_3BO_3, $MnCl_2 \cdot 4H_2O$,
186 $ZnCl_2$, $CoCl_2 \cdot 6H_2O$, $Na_2MoO_4 \cdot 2H_2O$, $CuCl_2 \cdot 2H_2O$, NaCl.
187 The algal growth inhibition test with *R. subcapitata*, formerly known as *Selenastrum capricornutum*
188 or *Pseudokirchneriella subcapitata*, was carried out as described in the ISO 8692 protocol (ISO,
189 2012). The growth of the algae exposed to the sample was compared with the growth of the algae in
190 a negative control. For each sample, six replicates were inoculated with 10^7 algal cells$\cdot l^{-1}$ in well
191 plates and incubated for 72 hrs at 23 ± 2 °C under continuous illumination (in an irradiance range of
192 120-60 µein$\cdot$ $m^{-2} \cdot s^{-1}$). The specific growth rate (µ) of *R. subcapitata* in each replicate was calculated
193 from the logarithmic increase in cell density in the interval 0-72 h as follows:
194 $$\mu = \frac{\ln N_i - \ln N_0}{t_i - t_0} \quad (1)$$
195 where N_0 and N_i represent the cell concentration at times t_0 and t_i respectively. Results were
196 expressed as the mean (± standard deviation) of the percentage inhibition of the cell growth
197 compared to the negative control.
198 The acute toxicity bioassay at 24 hours with *Daphnia magna* was conducted according to ISO 6341
199 (ISO, 2012). *D. magna* were selected from laboratory stock cultures, were moved in 2.0 l glass
200 beaker maintained at 24 ± 10 °C and were fed on *R. subcapitata*.
201 Twenty four hours before the test, adult daphnia were isolated and neonates produced from these
202 adults were used. For each test, four replicates each using 20 daphnids (<24 h old) were made. The

proportion of immobilised daphnids were recorded after 24 h. The test was considered valid if the immobilization in the control did not exceed 10%.

Negative and positive controls were included in each testing run. Negative tests were carried out on aqueous solutions containing 36 mM of hydrogen peroxide along with 90 µl of catalase (used with the aim of destroying residual hydrogen peroxide) per liter of solution.

Eco-toxicity data were expressed as the EC_{50} (median effect concentration) values and its 95% confidence intervals calculated by non-linear regression.

The significance of differences between mean values of experimental treatments and controls was assessed by Student's t-test and analysis of variance (ANOVA) with a 0.05 significance level. When ANOVA revealed significant differences among treatments, post-hoc analysis were carried on with Dunnett's method (Dunnett, 1955) and Tukey's test (Tukey, 1949). Statistical analyses were performed using Graphpad Prism software.

3. Results and discussions

3.1 Biodegradability assessment

In the tests with the inactivated sludge, it was firstly verified that the adsorption on them of the substrates investigated does not assume a significant role in their removal, according to Stolte *et al.* (Stolte, 2008).

For each tested compound, ten recharges were carried out until a constant biodegradation rate was observed. Among all the IM species studied, biodegradation was only seen for IMID.

In order to evaluate the first pseudo-order kinetic constant of biodegradation of Imid ($k_{bio/Imid}$), the $\ln(C/C_0)$ *vs* time was plotted (Figure 3), reaching a k_{bio} value equal to 0.24 h^{-1}. These results were in agreement to previous studies (Liwarska-Bizukojc et al., 2015; Liwarska-Bizukojc et al., 2014) in which it was found that the ILs with short alkyl side chains, such as 1E3MI and 1B3MI, are not biodegradable. Therefore, it is possible to assume that these compounds cannot be treated by conventional biological processes.

3.2 Direct UV_{254} photolysis

To evaluate the extent of direct photolysis of the four target compounds, they were individually submitted to the UV_{254} lamp photon flux in absence of hydrogen peroxide and at pH equal to 5.5 and 8.5.

After 2.0 h of irradiation, a 10-15% decrease of the initial substrates concentration ($[S]_0$ = 10 $mg \cdot l^{-1}$) was observed at both selected pHs (data not shown). The resistance of Imid, 1MI, 1E3MI, and 1B3MI to undergo UV_{254} photolysis can be mainly ascribed to the negligible molar absorption coefficient ($\varepsilon_{254}^{S_i}$) (Table 1).

On the basis of these results, and as reported previously (Stepnowski et al., 2005), it can be concluded that it is impossible to remove ionic liquids from wastewater in a municipal treatment plant equipped with a UV_{254} disinfection treatment unit alone. However, it is interesting to evaluate if the addition of small amounts of H_2O_2 during UV_{254} disinfection treatment may solve the problem, since it can promote the production of HO radicals, which are known to attack unselectively and rapidly the organic substances.

3.2. UV_{254}/H_2O_2 process

The UV_{254}/H_2O_2 process is frequently used as an AOP method for reducing contamination with biorefractory xenobiotics such as pharmaceuticals (Vogna et al., 2004; Andreozzi et al., 1999; Lopez et al., 2003), illicit drugs (Russo et al., 2016), dyes (Aleboyeh et al., 2012; Guimarães et al., 2012), pesticides (Semitsoglou-Tsiapou et al., 2016; Autin et al., 2013), chlorinated compounds (Kan et al., 2015; Pera-Titus et al., 2004), and so on. However, information is lacking on the kinetic constant values of the HO radical attack on the selected compounds ($k_{OH/Si}$).

To test the efficiency of the UV_{254}/H_2O_2 process on the removal of the imidazole-based compounds and, consequently, of estimating the unknown kinetic parameters, some experimental runs were carried out using combinations of different pH, substrate and H_2O_2 initial concentrations.

The $k_{OH/Si}$ values were estimated using a modified quantitative approach, which was successfully proposed for modelling the removal of phenolic compounds using the UV_{254}/H_2O_2 process (Alnaizy and Akergman, 2000). Particularly, UV_{254}/H_2O_2 process for the removal of the target compounds dissolved in bi-distilled water can be represented with a simplified kinetic scheme constituted by the reaction $r_{1\text{-}6}$ (Table 2). The process starts with the UV_{254} radiation absorption by H_2O_2 molecules, which undergo direct photolysis, leading to the formation of HO radicals (r_1). The latter can attack both the H_2O_2 molecules (r_2), generating the less reactive hydroperoxyl radicals, and the organic substrate (S_i) present into the solution (r_3). The chemical intermediates (BP), considered as pseudo-component and generated during the reaction r_3, can be further oxidized producing different BPs (r_4). Since 1B3MI and 1E3MI were dissolved as chloride salts, it is necessary to take into account also the consumption of HO radicals for the reaction with Cl^- ions deriving from ILs adding (r_5). Finally, the hydroperoxyl radicals produced through the reaction r_1 undergo a radical termination reaction to generate hydrogen peroxide (r_6).

Neglecting the direct UV_{254} photolysis of all the organic substrates and taking the steady-state hypothesis for the hydroxy and hydroperoxyl radicals, the consumption rates of the considered substrate, H_2O_2, and Cl^- ions can be expressed as follows ($eq_{1\text{-}3}$):

$$eq_1)\ \frac{d[S_i]}{dt} = -\frac{2\cdot k_{HO/S}\cdot[S_i]\cdot F_{H_2O_2}}{k_h\cdot[H_2O_2]+k_{HO/S}\cdot([S_i]+[BP])+k_{HO/Cl}\cdot[Cl^-]}$$

$$eq_2)\ \frac{d[H_2O_2]}{dt} = -F_{H_2O_2} - \frac{k_h\cdot[H_2O_2]\cdot F_{H_2O_2}}{k_h\cdot[H_2O_2]+k_{HO/S}\cdot([S_i]+[BP])+k_{HO/Cl}\cdot[Cl^-]}$$

$$eq_3)\ \frac{d[Cl^-]}{dt} = -\frac{2\cdot k_{HO/Cl}\cdot[Cl^-]\cdot F_{H_2O_2}}{k_h\cdot[H_2O_2]+k_{HO/S}\cdot([S_i]+[BP])+k_{HO/Cl}\cdot[Cl^-]}$$

where the term $F_{H_2O_2}$ represents the direct hydrogen peroxide photolysis rate. $F_{H_2O_2}$:

$$eq_4)\ F_{H_2O_2} = \frac{\Phi_{254}^{H_2O_2}\cdot I_0}{V}\cdot\left(1-exp\left(2.3\cdot z\cdot\varepsilon_{254}^{H_2O_2}\cdot[H_2O_2]\right)\right)$$

where $\Phi_{254}^{H_2O_2}$ and $\varepsilon_{254}^{H_2O_2}$ are the quantum yield of direct photolysis and the molar absorption coefficient for hydrogen peroxide at 254 nm (Table 2). In particular, in *eq₄* the radiation absorption at 254 nm of the selected compounds was neglected due to the low $\varepsilon_{254}^{S_i}$ values (Table 1)

The set of three ODEs constituted by the *eq₁*-*eq₃*, once integrated by means of the ode45 MATLAB routine, made it possible to predict the substrate and H_2O_2 concentration trends. The $k_{HO/Si}$ parameters were estimated minimizing the square of the differences between the calculated (*y*) and experimental (*c*) concentration of each species through an iterative optimization procedure (Reklaitis et al., 1983). Specifically, the objective function (Ω) was expressed as:

$$eq_5) \quad \Omega = \sum_{g=1}^{h} \sum_{i=1}^{l} \sum_{m=1}^{n} \left(y_{g,i,m} - c_{g,i,m}\right)^2$$

where *h*, *l* and *n* respectively represent the number of experimental data taken in each experiment, the number of the followed species in each experiment, and the number of the experiments considered in the optimization procedure.

The $k_{OH/Si}$ values, not previously reported in literature, estimated in this investigation by the numerical procedure were further validated by a competition kinetic procedure using BA as reference compound (Arouma et al., 1989; Buxton et al., 1988).

The mass balances necessary for the competition method implementation are those on S_i and BA:

$$eq_6) \frac{d[S_i]}{dt} = -k_{HO/S} \cdot [S_i] \cdot [HO^\bullet]$$

$$eq_7) \frac{d[BA]}{dt} = -k_{HO/BA} \cdot [BA] \cdot [HO^\bullet]$$

where $k_{HO/BA}$ represents the kinetic rate constant of the reaction between the HO radicals and BA and is equal to $5.9 \cdot 10^9$ $M^{-1} \cdot s^{-1}$ (Buxton et al, 1988; Onstein et al., 1999),.

When *eq₆* and *eq₇* are integrated, it is possible to obtain the following linear relation between the logarithms of the normalized target compound and BA concentrations:

$$eq_8) \ ln\left(\frac{[S_i]}{[S_i]_0}\right) = \frac{k_{HO/S_i}}{k_{HO/BA}} \cdot ln\left(\frac{[BA]}{[BA]_0}\right)$$

3.2.1. $k_{OH/Si}$ estimation

The initial experimental conditions of the experimental runs adopted during the optimization procedures, along with the percentage standard deviation (σ_i) on the imidazole-based compounds and H_2O_2, are shown in Table 3. In this regard, the percentage standard deviation on the i^{th}-species was evaluated as follows:

$$eq_9) \quad \sigma_i(\%) = \frac{1}{\bar{c}_i}\sqrt{\sum_{g=1}^{h}\frac{\left(y_{i,g}-c_{i,g}\right)^2}{h-p}}\cdot 100$$

where $\bar{c}_i$ represents the average measured concentration of the i^{th}-species and p is the number of the unknown parameters that have to be estimated. In this case, p was set equal to one, since $k_{HO/Si}$ represents the sole unknown parameter. As shown in Table 3, the model had good predictive power, since the percentage standard deviations on the investigated compounds and H_2O_2 were slightly lower than those associated with the experimental determination of these species (3-4%).

Since the kinetic constant of the reaction between $HO^{\bullet}$ and Imid ($k_{OH/Imid}$) was already reported in the literature at varying pH of the reacting solution, $k_{OH/Imid}$ was evaluated only through the numerical method. In fact, at pH = 7.4, two different $k_{OH/Imid}$ values were reported: $4.8\cdot10^9$ $M^{-1}\cdot s^{-1}$ (Arouma et al., 1989) and $6.4\cdot10^9$ $M^{-1}\cdot s^{-1}$ (Ching et al., 1993) both measured using the competition kinetic method with deoxyribose and HO radicals generated by a Fe(II)/EDTA/H_2O_2 reaction. Additionally, in a previous paper, two other $k_{OH/Imid}$ values were measured, by means of pulse radiolysis, at pH's of 6.8 and 10.9 and were shown to be $8.7\cdot10^9$ $M^{-1}\cdot s^{-1}$ and $1.2\cdot10^{10}$ $M^{-1}\cdot s^{-1}$ respectively (Rao et al, 1975). As reported in Table 4, the $k_{HO/Imid}$ values estimated in this investigation seem to agree with some of the previous findings. In particular the $k_{HO/Imid}$ value at pH equal to 8.5 ($4.42\cdot10^9$ $M^{-1}\cdot s^{-1}$) is very close to the value estimated at pH = 7.4 by Arouma et al. (1989). At the same time, the $k_{HO/Imid}$ value at pH equal to 5.5 ($2.33\cdot10^9$ $M^{-1}\cdot s^{-1}$) confirms that this kinetic constant increases with pH.

The kinetic constant of the reaction between HO radicals and 1MI ($k_{OH/1MI}$) measured by pulse radiolysis at pH's of 9.4 and 4.5 were shown to be $8.1 \cdot 10^9$ $M^{-1} \cdot s^{-1}$ and $5.0 \cdot 10^9$ $M^{-1} \cdot s^{-1}$ (Rao et al, 1975). Since these two values are the only ones reported in literature, both the direct and the competition kinetic methods were used for evaluating $k_{OH/1MI}$ values which are reported in Table 4 along with 95% confidence interval (CI) and the coefficients of determination (R^2). The results obtained with the competition kinetic method are close to those previously obtained at similar pH. As in the case of $k_{HO/Imid}$, and as previously reported for 1MI (Rao et al, 1975), the trend for $k_{HO/1MI}$ to increase at increasing pH is confirmed.

The differences of $k_{OH/Si}$ values for Imid and 1MI at two pHs could be tentatively ascribed to the higher reactivity of the un-protonated forms with respect to protonated forms with pK_a values 6.99 for Imid (Catalan and Elguero, 1984) and 7.33 for 1MI (Charton, 1965).

The comparison of $k_{OH/1B3MI}$ and $k_{OH/1E3MI}$ values at the two selected pH shows that the reaction rate between the HO radicals and the imidazolium-based ILs increase with increasing alkyl chain length, as recently reported for the same ILs (Domínguez et al., 2014). The increase in reactivity of the HO radical with the lengthening of the substituent of the imidazolium ionic liquid at position 1-N could be due to the presence of a higher number of oxidizable centers at greater lengths.

3.2.2. Validation of the proposed model and the values of kinetic parameter estimated

With the aim of validating the mathematical model, the results of fourteen additional photocatalytic runs, carried out using different S_i and H_2O_2 initial concentrations (Table 5), were compared with the model predictions without any further adjustment of the previously estimated parameters ($k_{HO/Si}$). The model was predictive for the observed behavior of the system as shown by the percentage standard deviation values on the investigated species and H_2O_2. This conclusion can also be confirmed, on a qualitative basis, by a visual comparison of the calculated and experimental concentration data for all the measured species involved in the process. For this purpose, the S_i and

346 H_2O_2 theoretical and experimental concentrations of some experimental runs used for the validation
347 procedure were reported in Figure 4.
348
349 **3.3. Eco-toxicity assessment**
350 The "effect-driven approach" (Escher and Fenner, 2011), in which a compound is degraded and is
351 analyzed with eco-bioassays, was used to follow the eco-toxicity evolution of the selected
352 imidazolium based compounds during the UV_{254}/H_2O_2 process.
353 Ecotoxicological tests were performed on samples collected from UV_{254}/H_2O_2 experiments
354 performed in the cylindrical batch reactor with an aqueous solution containing one of the substrates
355 and H_2O_2 at initial concentrations of 150 $mg \cdot l^{-1}$ and 1224 $mg \cdot l^{-1}$ ($36 \cdot 10^{-3}$ M) respectively. The
356 1E3MI and 1B3MI initial concentration of 150 $mg \cdot l^{-1}$ were calculated for the ionic species ($1E3MI^+$
357 and $1B3MI^+$) without taking into consideration the contribution of chloride ions. As reported in
358 previous studies (Postigo et al., 2011; An et al., 2015; Xu et al., 2014), such high initial substrate
359 concentrations were chosen to better assess ecotoxicologial effects of photogenerated by-products
360 and to determine the median effective concentration (EC_{50}) of the selected substrates.
361 In addition to the sample collected at baseline (t_0), two further samples were collected at a reaction
362 time (t_f) corresponding to almost complete substrate conversion and at double that time ($2t_f$) The
363 samples taken at $2t_f$ were deemed to be representative of a solution expected to contain secondary
364 oxidation by-products. Within the reaction range chosen, TOC and COD analysis evidenced a
365 noticeable mineralization phenomenon, as reported in Table 6.
366 The results of ecotoxicological tests with *D. magna* and *R. subcapitata* in the presence of imidazole,
367 1-methyl-imidazole, 1-ethyl-3-methyl-imidazolium, and 1-butyl-3-methyl-imidazolium chlorides
368 contaminated solutions are shown in Table 7.
369 Results with *D. magna* and *R. subcapitata* showed that the relative toxicity order was $1B3MI^+$ >
370 $1MI \approx 1E3MI^+$ > Imid. In particular, the EC_{50} of $1B3MI^+$ was estimated as 70.4 µM and 249 µM for
371 *D. magna* and *R. subcapitata* respectively. The EC_{50} values of 1MI and $1E3MI^+$, measured with the

same organisms, are one order of magnitude higher than those evaluated for $1B3MI^+$. Finally, the EC_{50} values of Imid measured with *D. magna* and *R. subcapitata* are even greater than those of 1MI and $1E3MI^+$. These results agree with published findings that the negative effect of ionic liquids on biological systems increases with lengthening alkyl chains (Petkovic et al., 2011; D. Demberelnyamba et al., 2004). Additionally, the EC_{50} values, measured here with $1E3MI^+$ and $1B3MI^+$ are very close to those previously evaluated (Table 7).

In general, when compared to *R. subcapitata*, *D.magna* was more sensitive to Imid, 1MI, 1E3MI and 1B3MI solutions, as shown in Table 7. The mechanism of toxicity of IMI-ILs towards *D.magna* remains unknown but several studies have suggested destabilization of membrane permeability, defense enzyme activity and structural damage to the DNA, as possible contributors to IMI-ILs toxicity to *D.magna* (Samorì et al., 2010; Luo et al., 2008).

On the basis of the EU-Directives 93/67/ECC (EC 1996), the hazard rankings of the four selected substances were also reported in Table 7 by their EC_{50} values (whereby $EC_{50} < 1.0$ mg·l^{-1} is deemed 'very toxic to aquatic organisms'; 1.0–10 mg·l^{-1} are 'toxic to aquatic organisms' and 10–100 mg·l^{-1} are classified as 'harmful to aquatic organisms' and chemicals with an EC_{50} above 100 mg·l^{-1} are not classified).

The results of 24 h immobilization tests with *D. magna* in contact with t_0, t_f and $2t_f$ samples at varying the dilution factor are displayed in Figure 5. We observed that the t_f treated samples notably showed almost the same toxicity as the t_0 sample (untreated) on *D. magna*, except for the UV_{254}/H_2O_2 treated 1E3MI containing solution. In fact, when the solution containing $1E3MI^+$, at the initial concentration of 150 mg·l^{-1}, undergoes the proposed treatment duration equal to t_f, a dilution factor of the treated solution equal to $6.2 \cdot 10^{-2}$, allows for a 50% immobilization frequency. By contrast, the EC_{50} of $1E3MI^+$ on *D. magna*, the t_0 untreated solution needs a dilution factor equal to only $4.2 \cdot 10^{-1}$ to generate the same immobilization frequency. Nevertheless, toxicity was significantly reduced when daphnids were exposed to $2t_f$ samples of all tested compounds, thus demonstrating that the secondary oxidation by-products did not affect the mobility of *D. magna*.

When the toxicity on *R. subcapitata* of t_f and $2t_f$ samples at varying dilution factor was studied, somewhat different results from those achieved with *D. magna* were obtained. As shown in Figure 6, both t_f and $2t_f$ diluted samples, deriving from UV_{254}/H_2O_2 treatment of $1E3MI^+$ and $1B3MI^+$ solutions had a toxicity higher than t_0 diluted sample. In particular, for t_f and $2t_f$ samples collected from treated $1B3MI^+$ solutions, the dilution factors needed to produce a 50% inhibition of algal grow rate are close to $1.4 \cdot 10^{-1}$. This dilution factor is almost half of that necessary to obtain the same inhibition of growth rate by diluting the t_0 sample ($2.3 \cdot 10^{-1}$). For t_f and $2t_f$ samples of treated $1E3MI^+$ solutions, the dilution factors that lead to a 50% inhibition of algal growth rate are equal to $2.4 \cdot 10^{-1}$ and $4.9 \cdot 10^{-1}$ respectively. In this case, the increasing in toxicity, due to the UV_{254}/H_2O_2 treatment, is even more pronounced since the untreated t_0 solution should be concentrated 2.4 times to inhibit the algal growth of 50%.

An increase in toxicity of the UV_{254}/H_2O_2 treated solutions has already been reported. In fact, in recent papers it was noted that some by-products are even more toxic than their parent drugs as in the case of the direct UV_{254} photolysis and UV_{254}/H_2O_2 treatment of oxytetracycline, doxycycline, ciprofloxacin, and fenofibric acid (Yuan et al., 2011; Santiago et al., 2011). This means that a decrease of COD and TOC (Table 7) does not always correspond to a consequent decrease in toxicity of the compounds.

Conclusion

The removal of Imid, 1MI, 1E3MI and 1B3MI from contaminated aqueous solutions was effectively carried out by means of the UV_{254}/H_2O_2 advanced oxidation process. By contrast, both aerobic biological oxidation and direct UV_{254} photolysis are not able to remove the four target compounds except in the case of Imid biodegradation, which is characterized by a $k_{bio/Imid}$ equal to $0.24\ h^{-1}$.

With the aim of providing useful data for the design of a UV_{254}/H_2O_2 treatment unit for the removal of the selected compounds, the data we generated were used for the determination of the $k_{OH/Si}$ at

both selected pHs (numerical method). The $k_{OH/Si}$ values were shown to be between $2.32 \cdot 10^9$ $M^{-1} \cdot s^{-1}$ and $5.52 \cdot 10^9$ $M^{-1} \cdot s^{-1}$. Moreover, in accordance with previous findings on Imid and 1MI, the data we obtained confirmed a dependency of $k_{OH/Si}$ with pH and Imid and 1MI pK_a values. Since very little and mainly dated information was found on the $k_{OH/Si}$ of 1MI, 1E3MI, and 1B3MI, these kinetic constants were evaluated using the competition kinetic method with benzoic acid as a reference compound. Reasonable agreement of $k_{OH/Si}$ values estimated with the two methods was found at both pHs. The validation procedure also demonstrated that the model had good predictive ability for the behavior of the system.

Ecotoxicity assessments conducted using *R. subcapitata* and *D. magna*, and solutions contaminated with the target compounds before and after the UV_{254}/H_2O_2 treatment showed three interesting findings: i) in accordance with previous literature findings, 1E3MI and 1B3MI should be considered harmful and toxic to aquatic organisms; ii) the toxicity of N,N'-alkyl-imidazolium salts increases at increasing alkyl chain length; iii) the 1E3MI and 1B3MI by-products deriving from the UV/H_2O_2 process are even more toxic than the target compounds.

Acknowledgments

This research was carried under the framework of the Project "Emerging contaminants in soil and water: from source to marine environment" funded by the Italian Ministry of Education, University and Research (MIUR) in the context of the Research Programme of National Interest (PRIN) 2010-2011.

References

Aleboyeh, A., Kasiri, M.B., Aleboyeh, H., 2012. Influence of dyeing auxiliaries on AB74 dye degradation by UV/H2O2 process. J. Environ. Manage. 113, 426–431.

448 Alnaizy, R., Akergman, A., 2000. Advanced oxidation of phenolic compounds. Adv. Environ. Res.
449 4, 233–244.
450 An, T., An, J., Gao, Y., Li, G., Fanga, H., Song, W., 2015. Photocatalytic degradation and
451 mineralization mechanism and toxicity assessment of antivirus drug acyclovir: Experimental and
452 theoretical studies. Appl. Catal., B 164, 279–287.
453 Anderson, E.B., Long, T.E., 2010. Imidazole- and imidazolium-containing polymers for biology
454 and material science applications. Polymer 51, 2447–2454.
455 Andreozzi, R., Cesaro, R., Marotta, R., Pirozzi, F., 2006. Evaluation of biodegradation kinetic
456 constants for aromatic compounds by means of aerobic batch experiments. Chemosphere. 62 1431–
457 1436.
458 Andreozzi, R., Caprio, V., Insola, A., Marotta, R., 1999. Advanced oxidation processes (AOP) for
459 water purification and recovery. Catalysis Today 53 (1), 51–59.
460 APHA, AWWA, WEF. Standard methods for the examination of water and wastewater 21st ed, 21
461 st, Washington, 2005.
462 Arouma, O.I., Laughton, M.J., Halliwell, B., 1989. Carnosine, homocarnosine and anserine: could
463 they act as antioxidants in vivo?. Biochem. J. 264, 863-869.
464 Autin, O., Hart, J., Jarvis, P., MacAdam, J., Parsons, S.A., Jefferson, B., 2013. The impact of
465 background organic matter and alkalinity on the degradation of the pesticide metaldehyde by two
466 advanced oxidation processes: UV/H2O2 and UV/TiO2, Water Res. 47, 2041–2049.
467 Bernot, R.J., Brueseke, M.A., Evans-White, M.A., Lamberti, G.A., 2005. Acute and chronic
468 toxicity of imidazolium-based ionic liquids on Daphnia magna. Environ. Toxicol. Chem. 24, 87–92.
469 Biczak, R., Pawlowska, B., Balczewski, P., Rychter, P, 2014. The role of the anion in the toxicity of
470 imidazolium ionic liquids. J. Hazard. Mater. 274, 181– 190.
471 Bielski, B.H., Cabelli, D.E., Aruda, R.L., Ross, A.B., 1985. Reactivity of HO2/O2 radicals in
472 aqueous solution. J. Phys. Chem. Ref. Data 14, 1041–1077.

473 Bocos, E., Pazos, M., Sanromàn, M.A., 2016. Electro-Fenton treatment of imidazolium-based ionic
474 liquids: kinetics and degradation pathways. RSC Adv. 6, 1958–1965.
475 Bubalo, M.C., Radošević, K., Redovniković, I.R., Halambek, J., Srček, V.G., 2014. A brief
476 overview of the potential environmental hazards of ionic liquids. Ecotox. Environ. Safe. 99, 1–12.
477 Buxton, G.V., Greenstock, C.L., Helman, W.P., Ross, A.B., 1988. Critical review of rate constants
478 for reactions of hydrated electrons, hydrogen atoms and hydroxyl radicals (OH/O) in aqueous
479 solution. J. Phys. Chem. Ref. Data 17, 513–886.
480 Catalan, J., Elguero, J., 1984. Basicity of azoles. IV. Empirical relationships between basicity and
481 ionization potential for aromatic five membered rings containing nitrogen or oxygen. J. Heterocycl.
482 Chem. 21 (1), 269–270.
483 Charton, M., 1965. Electrical Effects of ortho substituents in imidazoles and benzimidazoles. J. Org.
484 Chem. 30 (10), 3346–3350.
485 Ching, T.L., Haenen, G.R.M.M., Bast, A., 1993. Cimetidine and other H2 receptor antagonists as
486 powerful hydroxyl radical scavengers. Chem.-Biol. Interactions 86, 119–127.
487 Cho, C.W., Jeon, Y.C., Pham, T.P., Vijayaraghavan, K., Yun, Y.S., 2008. The ecotoxicity of ionic
488 liquids and traditional organic solvents on microalga Selenastrum capricornutum. Ecotox. Environ.
489 Safe. 71, 166–171.
490 Couling, D.J., Bernot, R.J., Docherty, K.M., Dixon, J.K., Maginn, E.J., 2006. Assessing the factors
491 responsible for ionic liquid toxicity to aquatic organisms via quantitative structure-property
492 relationship modeling. Green Chem. 8, 82–90.
493 Czerwicka, M., Stolte, S., Müller, A., Siedlecka, E.M., Gołebiowski, M., Kumirska, J., Stepnowski,
494 P., 2009. Identification of ionic liquid breakdown products in an advanced oxidation system. J.
495 Hazard. Mater. 171, 478–483.
496 Demberelnyamba, D., Kim, K.S., Choi, S., Park, S.Y., Lee, H., Kimb C.J., Yoob, I.D., 2004.
497 Synthesis and antimicrobial properties of imidazolium and pyrrolidinonium salts. Bioorg. Med.
498 Chem. 12, 853–857.

499 Domínguez, C.M., Munoz, M., Quintanilla, A., de Pedro, Z.M., Ventura, S.P.M., Coutinho, J.A.P.,
500 Casas, J.A., Rodriguez, J.J., 2014. Degradation of imidazolium-based ionic liquids in aqueous
501 solution by Fenton oxidation. J. Chem. Technol. Biotechnol. 89, 1197–1202.
502 Dunnett C.W., 1955. A multiple comparison procedure for comparing several treatments with a
503 control. J. Amer. Statist. Assoc. 50, 1096–1121
504 Dupont, J., Suarez, P.A.Z., 2006. Physico-chemical processes in imidazolium ionic liquids. Phys.
505 Chem. Chem. Phys. 8, 2441–2452.
506 EC 1996. Technical Guidance Document in support of the Commission Directive 93/67/EEC on
507 Risk Assessment for New Notified Substances and Commission Regulation (EC) No 1488/94 on
508 Risk Assessment for Existing Substances. Parts 1-4. Office for Official Publications of the EC,
509 Luxembourg, 1996.
510 Escher, B.I., Fenner, K., 2011. Recent advances in environmental risk assessment of transformation
511 products. Environ. Sci. Technol. 45, 3835–3847.
512 Garcia, M.T., Gathergood, N., Scammells, P.J., 2005. Biodegradable ionic liquids Part II. Effect of
513 the anion and toxicology. Green Chem. 7, 9–14.
514 Goldstein, S., Aschengrau, D., Diamant, Y., Rabani, J., 2007. Photolysis of aqueous H2O2:
515 quantum yield and applications for polychromatic UV actinometry in photoreactors. Environ. Sci.
516 Technol. 41, 7486–7490.
517 Guimarães, J.R., Maniero, M.G., Nogueira de Araújo, R., 2012. A comparative study on the
518 degradation of RB-19 dye in an aqueous medium by advanced oxidation processes. J. Environ.
519 Manage. 110, 33–39.
520 Haag, W., Yao, C., 1992. Rate constants for reaction of hydroxyl radicals with several drinking
521 water contaminants. Environ. Sci. Technol. 26, 1005–1013.
522 ISO 6341, 2012. Water quality - Determination of the inhibition of the mobility of Daphnia magna
523 Straus (Cladocera, Crustacea) - Acute toxicity test, n.d.

524 ISO 8692, 2012. Water quality - Fresh water algal growth inhibition test with unicellular green
525 algae, n.d.
526 Jastorff, B., Mölter, K., Behrend, P., Bottin-Weber, U., Filser, J., Heimers, A., Ondruschka, B.,
527 Ranke, J., Schaefer, M., Schröder, H., Stark, A., Stepnowski, P., Stock, F., Störmann, R., Stolte, S.,
528 Welz-Biermann, U., Ziegert, S., Thöming, J., 2005. Progress in evaluation of risk potential of ionic
529 liquids-basis for an eco-design of sustainable products. Green Chem. 7, 362–372
530 Jordan, A., Gathergood, N., 2015. Biodegradation of ionic liquids – a critical review. Chem. Soc.
531 Rev. 44, 8200–8237.
532 Kan, E., Koh, C.I., Lee, K., Kang, J., 2015. Decomposition of aqueous chlorinated contaminants by
533 UV irradiation with H2O2. Front. Environ. Sci. Eng. 9 (3), 429–435.
534 Kumar, J.R., 2010. Review of imidazole heterocyclic ring containing compounds with their
535 biological activity. Pharmacophore 1(3), 167–77.
536 Liwarska-Bizukojc, E., Maton, C., Stevens, C.V., 2015. Biodegradation of imidazolium ionic
537 liquids by activated sludge microorganisms. Biodegradation 26, 453–463.
538 Liwarska-Bizukojc, E., Maton, C., Stevens, C.V., Gendaszewska, D., 2014. Biodegradability and
539 kinetics of the removal of new peralkylated imidazolium ionic liquids. J. Chem. Technol.
540 Biotechnol. 89, 763–768.
541 Lopez, A., Bozzi, A., Mascolo, G., Kiwi, J., 2003. Kinetic investigation on UV and UV/H2O2
542 degradations of pharmaceutical intermediates in aqueous solution. J. Photochem. Photobiol., A 156,
543 121–126.
544 Luo, Y.R., Li, X.Y., Chen, X.X., Zhang, B.J., Sun, Z.J., Wang, J.J., 2008. The developmental
545 toxicity of 1-methyl-3-octylimidazolium bromide on Daphnia magna. Environ. Toxicol. 23 (6),
546 736–44.
547 Matzke, M., Stolte, S., Arning, J., Uebers, U., Filser, J., 2008. Imidazolium based ionic liquids in
548 soils: Effects of the side chain length on wheat (Triticum aestivum) and cress (Lepidium sativum)
549 as affected by different clays and organic matter. Green Chem. 10, 584–591

550 Matzke, M., Stolte, S., Thiele, K., Juffernholz, T., Arning, J., Ranke, J., Welz-Biermann, U.,
551 Jastorff, B., 2007. The influence of anion species on the toxicity of 1-alkyl-3-methylimidazolium
552 ionic liquids observed in an (eco)toxicological test battery. Green Chem. 9 (11), 1198−1207.
553 Munoz, M., Domínguez, C.M., de Pedro, Z.M., Quintanilla, A., Casas, J.A., Ventura, S.P.M.,
554 Coutinho, J.A.P., 2015. Role of the chemical structure of ionic liquids in their ecotoxicity and
555 reactivity towards Fenton oxidation. Sep. Purif. Technol. 150, 252–256.
556 Onstein, P., Stefan, M.I., Bolton, J.R., 1999. Competition kinetics method for the determination of
557 rate constants for the reaction of hydroxyl radicals with organic pollutants using the UV/H2O2
558 advanced oxidation technology: the rate constants for the tert-buthyl formate ester and 2,4-
559 dinitrophenol. J. Adv. Oxid. Technol. 4 (2), 231–236.
560 Pera-Titus, M., Garcia-Molina, V., Banos, M.A., Gimenez, J., Esplugas, S., 2004. Degradation of
561 chlorophenols by means of advanced oxidation processes: a general review. Appl. Catal., B 47 (4),
562 219–256.
563 Peric, B., Sierra, J., Marti, E., Cruanas, R., Garau, M.A., 2014. A comparative study of the
564 terrestrial ecotoxicity of selected protic and aprotic ionic liquids. Chemosphere 108, 418– 425.
565 Petkovic, M., Seddon, K.R., Rebelo, L.P.N., Pereira, C.S., 2011. Ionic liquids: A pathway to
566 environmental acceptability. Chem. Soc. Rev. 40, 1383–1403
567 Pham, T.P.T., Cho, C.-W., Min, J., Yun, Y.-S., 2008. Alkyl-chain length effects of imidazolium and
568 pyridinium ionic liquids on photosynthetic response of Pseudokirchneriella subcapitata. J. Biosci.
569 Bioeng. 105, 425–428.
570 Postigo, C., Sirtori, C., Ollerb, I., Malato, S., Maldonado, M.I., de Aldaa, M.L., Barceló, D., 2011.
571 Solar transformation and photocatalytic treatment of cocaine in water: Kinetics, characterization of
572 major intermediate products and toxicity evaluation. Appl. Catal., B 104, 37–48.
573 Rao, P.S., Simic, M., Hayon, E., 1975. Pulse radiolysis study of imidazole and histridine in water. J.
574 Phys. Chem. 79, 1260–3.
575 Reklaitis, G.V., Ravindran, A., Regsdell, K.M., Engineering Optimization, Wiley, New York, 1983.

576 Richardson, S.D., Ternes, T.A., 2014. Water Analysis: Emerging Contaminants and Current Issues.
577 Anal. Chem. 86, 2813−2848.
578 Romero, A., Santos, A., Tojo, J., Rodrìguez, A., 2008. Toxicity and biodegradability of
579 imidazolium ionic liquids. J. Hazard. Mater. 151, 268–273.
580 Rosenfeldt, E.J., Linden, K.G., Canonica, S., von Gunten, U., 2006. Comparison of the efficiency of
581 •OH radical formation during ozonation and the advanced oxidation processes O3/H2O2 and
582 UV/H2O2. Water Res. 40, 3695–3704.
583 Russo, D., Spasiano, D., Vaccaro, M., Cochran, K.H., Richardson, S.D., Andreozzi, R., Li Puma,
584 G., Reis, N.M., Marotta, R., 2016. Investigation on the removal of the major cocaine metabolite
585 (benzoylecgonine) in water by UV254/H2O2, process by using a flow microcapillary film array
586 photoreactor as an efficient experimental tool. Water Res. 89, 375–383.
587 Samorì, C., Malferrari, D., Valbonesi, P., Montecavalli, A., Moretti, F., Galletti, P., Sartor, G.,
588 Tagliavini, E., Fabbri, E., Pasteris, A., 2010. Introduction of oxygenated side chain into
589 imidazolium ionic liquids: evaluation of the effects at different biological organization levels.
590 Ecotoxicol. Environ. Saf. 73, 1456–1464.
591 Semitsoglou-Tsiapou, S., Templeton, M.R., Graham, N.J.D., Leal, L.H., Martijn, B.J., Royce, A.,
592 Kruithof, J.C., 2016. Low pressure UV/H2O2 treatment for the degradation of the pesticides
593 metaldehyde, clopyralid and mecoprop e Kinetics and reaction product formation. Water Res. 91,
594 285–294.
595 Santiago, J., Agüera, A., Gómez-Ramos, M.d.M., Fernández Alba, A.R., García-Calvo, E., Rosal,
596 R., 2011. Oxidation by-products and ecotoxicity assessment during the photodegradation of
597 fenofibric acid in aqueous solution with UV and UV/H2O2. J. Hazard. Mater. 194, 30–41.
598 Siedlecka, E.M., Gołebiowski, M., Kaczynski, Z., Czupryniak, J., Ossowski, T., Stepnowski, P.,
599 2009. Degradation of ionic liquids by Fenton reaction; the effect of anions as counter and
600 background ions. Appl. Catal., B 91, 573–579.

601 Siedlecka, E.M., Mrozik, W., Kaczynski, Z., Stepnowski, P., 2008. Degradation of 1-butyl-3-
602 methylimidazolium chloride ionic liquid in a Fenton-like system. J. Hazard. Mater. 154, 893–900.
603 Stepnowski, P., Zaleska, A., 2005. Comparison of different advanced oxidation processes for the
604 degradation of room temperature ionic liquids. J. Photochem. Photobiol., A 170, 45–50.
605 Steudte, S., Stepnowski, P., Cho, C-W., Thöming, J., Stolte, S., 2012. (Eco)toxicity of fluoro-
606 organic and cyano-based ionic liquid anions. Chem. Commun. 48, 9382–9384.
607 Stolte, S., Abdulkarim, S., Arning, J., Blomeyer-Nienstedt, A.-K., Bottin-Weber, U., Matzke, M.,
608 Ranke, J., Jastorff, B., Thoming, J., 2008. Primary biodegradation of ionic liquid cations,
609 identification of degradation products of 1-methyl-3-octylimidazolium chloride and electrochemical
610 wastewater treatment of poorly biodegradable compounds. Green Chem. 10, 214–224.
611 Tukey, J. W., 1949. Comparing individual means in the analysis of variance. Biometrics 5, 99–114.
612 Ullmann's Encyclopedia of Industrial Chemistry, sixth ed. Wiley-VCH, Weinheim, 2005.
613 Urano, K., Kato, Z., 1986. A method to classify biodegradabilities of organic compounds. J.
614 Hazard. Mater. 13, 135–145.
615 Vogna, D., Marotta, R., Andreozzi, R., Napolitano, A., d'Ischia, M., 2004. Kinetic and chemical
616 assessment of the UV/H2O2 treatment of antiepileptic drug carbamazepine. Chemosphere 54, 497–
617 505.
618 Wells, A.S., Coombe, V.T., 2006. On the freshwater ecotoxicity and biodegradation properties of
619 some common ionic liquids. Org. Pro. Res. Dev. 10, 794–798.
620 Wu, X., Tong, Z.H., Li, L.L., Yu, H.Q, 2013. Toxic effects of imidazolium-based ionic liquids on
621 Caenorhabditis elegans: The role of reactive oxygen species. Chemosphere 93 (10), 2399−2404.
622 Xu, J., Hao, Z., Guo, C., Zhang, Y., He, Y., Meng, W., 2014. Photodegradation of sulfapyridine
623 under simulated sunlight irradiation: Kinetics, mechanism and toxicity evolvement. Chemosphere
624 99, 186–191.
625 Yuan, F., Hu, C., Hu, X., Wei, D., Chen, Y., Qu, J., 2011. Photodegradation and toxicity changes of
626 antibiotics in UV and UV/H2O2 process. J. Hazard. Mater. 185, 1256–1263.

627 Zhang, Z., Chen, S., Li, Y., Li, S., Wang, L., 2009. A study of the inhibition of iron corrosion by
628 imidazole and its derivatives self-assembled films. Corrosion Science 51, 291–300.

Table

Click here to download Table: tables.docx

	Imid	**1MI**	**1E3MI**	**1B3MI**
$\varepsilon_{254}^{S_i}$ (10^{-6} M^{-1} cm^{-1})	2.8	2.3	4.6	2.4

Table 1

r_1)	$H_2O_2 \xrightarrow{h\nu} 2HO^{\bullet}$	$\Phi_{254}^{H_2O_2} = 0.55$ mol ein^{-1} $\varepsilon_{254}^{H_2O_2} = 18.6\ M^{-1}\ cm^{-1}$	Goldstein et al. (2007)
r_2)	$HO^{\bullet} + H_2O_2 \xrightarrow{k_h} H_2O + HO_2^{\bullet}$	$k_h = 2.7 \cdot 10^7\ M^{-1}s^{-1}$	Buxton et al. (1988)
r_3)	$S_i + HO^{\bullet} \xrightarrow{k_{HO/S_i}} BP$	k_{HO/S_i} = unknown	(estimated in this work)
r_4)	$BP + HO^{\bullet} \xrightarrow{k_{HO/BP}} BP$	$k_{HO/BP} \approx k_{HO/S_i}$	(assumed in this work)
r_5)	$Cl^- + HO^{\bullet} \xrightarrow{k_{HO/Cl}} ClOH^-$	$k_{HO/Cl} = 4.3 \cdot 10^9\ M^{-1}s^{-1}$	Buxton et al. (1988)
r_6)	$2HO_2^{\bullet} \xrightarrow{k_t} H_2O_2 + O_2$	$k_t = 8.3 \cdot 10^5 M^{-1}s^{-1}$	Bielski et al., (1985)

Table 2

		$[S_i]_0$ (10^{-3} M)	$[H_2O_2]_0$ (10^{-3} M)	pH	σ_{Si} (%)	$\sigma_{H_2O_2}$ (%)
IMID	**run1**	0.143	16.5	5.5	0.75	0.20
	run2	0.142	17.7	8.5	0.88	0.28
1MI	**run3**	0.158	18.7	5.5	0.25	0.12
	run4	0.085	4.3	5.5	0.28	0.56
	run5	0.131	16.0	8.5	1.58	0.19
	run6	0.131	8.9	8.5	0.95	0.97
	run7	0.067	4.5	8.5	0.11	1.72
1E3MI	**run8**	0.099	16	5.5	1.61	0.19
	run9	0.096	8.4	5.5	1.81	0.06
	run10	0.099	17	8.5	0.73	0.56
	run11	0.085	8.5	8.5	1.46	0.20
1B3MI	**run12**	0.077	17	5.5	0.46	0.13
	run13	0.120	8.8	5.5	0.91	0.38
	run14	0.081	16	8.5	0.28	0.12
	run15	0.131	8.1	8.5	0.33	0.92

Table 3

	Numerical method		Competition kinetic method*		Literature findings		
	pH=5.5	**pH=8.5**	**pH=5.5**	**pH=8.5**	**$k_{OH/Si}$ ($M^{-1}\cdot s^{-1}$)**	**pH**	**Ref**
$k_{OH/Imid}$ ($M^{-1}\cdot s^{-1}$) **CI ($M^{-1}\cdot s^{-1}$)**	$2.33\cdot10^{9}$ $2.3\cdot10^{8}$	$4.42\cdot10^{9}$ $3.8\cdot10^{8}$	- -	- -	$4.8\cdot10^{9}$ $6.4\cdot10^{9}$ $8.7\cdot10^{9}$ $1.2\cdot10^{10}$	7.4 7.4 6.8 10.9	§ † ‡ ‡
$k_{OH/1MI}$ ($M^{-1}\cdot s^{-1}$) **CI ($M^{-1}\cdot s^{-1}$)** **R^2**	$2.32\cdot10^{9}$ $2.3\cdot10^{8}$ -	$4.25\cdot10^{9}$ $6.3\cdot10^{8}$ -	$3.92\cdot10^{9}$ - 0.99	$6.32\cdot10^{9}$ - 0.98	$5.0\cdot10^{9}$ $8.1\cdot10^{9}$	4.5 9.4	‡ ‡
$k_{OH/1E3MI}$ ($M^{-1}\cdot s^{-1}$) **CI ($M^{-1}\cdot s^{-1}$)** **R^2**	$3.43\cdot10^{9}$ $3.3\cdot10^{8}$ -	$3.69\cdot10^{9}$ $2.3\cdot10^{8}$ -	$2.91\cdot10^{9}$ - 0.98	$2.72\cdot10^{9}$ - 0.99			
$k_{OH/1B3MI}$ ($M^{-1}\cdot s^{-1}$) **CI ($M^{-1}\cdot s^{-1}$)** **R^2**	$4.49\cdot10^{9}$ $4.7\cdot10^{8}$ -	$5.52\cdot10^{9}$ $5.8\cdot10^{8}$ -	$3.90\cdot10^{9}$ - 0.99	$5.11\cdot10^{9}$ - 0.98			

Table 4

		$[S_i]_0$ (10^{-3} M)	$[H_2O_2]_0$ (10^{-3} M)	pH	σ_{Si} (%)	$\sigma_{H_2O_2}$ (%)
IMID	**run1s**	0.127	8.9	5.5	0.45	0.45
	run2s	0.070	17.6	8.5	1.62	0.14
1MI	**run3s**	0.155	8.7	5.5	1.67	1.01
	run4s	0.115	4.4	5.5	1.07	1.69
	run5s	0.148	4.1	8.5	0.74	1.55
	run6s	0.118	2.0	8.5	0.18	0.28
1E3MI	**run7s**	0.091	5.2	5.5	0.17	0.18
	run8s	0.093	2.3	5.5	1.07	0.40
	run9s	0.082	4.5	8.5	0.12	1.00
	run10s	0.081	2.4	8.5	0.10	0.30
1B3MI	**run11s**	0.050	4.1	5.5	0.11	0.73
	run12s	0.063	1.8	5.5	0.23	0.76
	run13s	0.063	3.9	8.5	1.22	0.36
	run14s	0.057	1.9	8.5	0.71	0.76

Table 5

	t_f (min)	$2t_f$ (min)	TOC/TOC$_0$ (%)		COD/COD$_0$ (%)	
			t_f	$2t_f$	t_f	$2t_f$
Imid	41	82	76	58	60	44
1MI	33	66	77	59	66	50
1E3MI	27	54	90	63	69	44
1B3MI	21	42	92	78	78	62

Table 6

	Species	Endpoint measured	EC_{50} (CI 95%) (µM)	Reference	Hazard ranking[a]
Imid	*R. subcapitata*	72h	14700 (13500-16200)	in this study	*
	D.magna	24 h	2140 (1850-2440)	in this study	*
1MI	*R. subcapitata*	72 h	3480 (2950-4090)	in this study	*
	D.magna	24 h	524 (414-670)	in this study	**
1E3MI$^+$	*R. subcapitata*	72 h	2730 (2520-2990)	in this study	*
	D.magna	24 h	774	Steudte et al. (2012)	**
			567 (441 -639)	in this study	**
1B3MI$^+$	*R. subcapitata*	96 h	277	Wells and Coombe (2006)	**
		72 h	249 (223-287)	in this study	**
	D.magna	48 h	84.8	Bernot et al. (2005) Couling et al. (2006)	**
			46.7	Wells and Coombe (2006)	***
		24 h	70.8	Garcia et al. (2005)	***
			70.4 (50.3-79.0)	in this study	***

Table 7

Figure

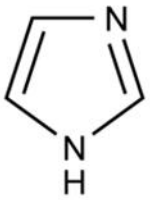

Imidazole (Imid)

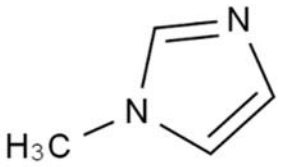

1-methylimidazole (1MI)

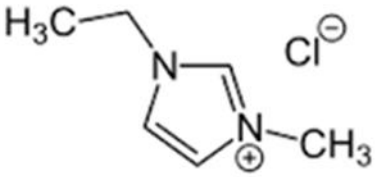

1-ethyl-3-methylimidazolium chloride (1E3MI)

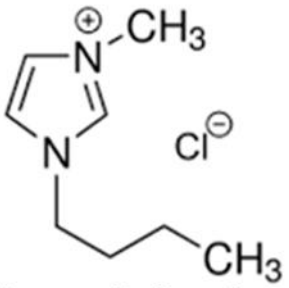

1-butyl-3-methylimidazolium chloride (1B3MI)

Figure 1

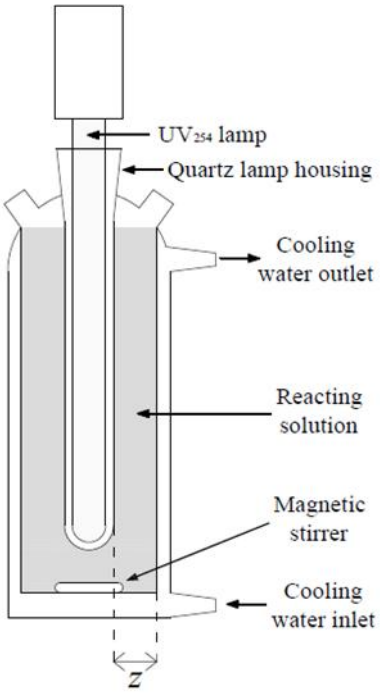
UV254 lamp
Quartz lamp housing
Cooling water outlet
Reacting solution
Magnetic stirrer
Cooling water inlet
z

Figure 2

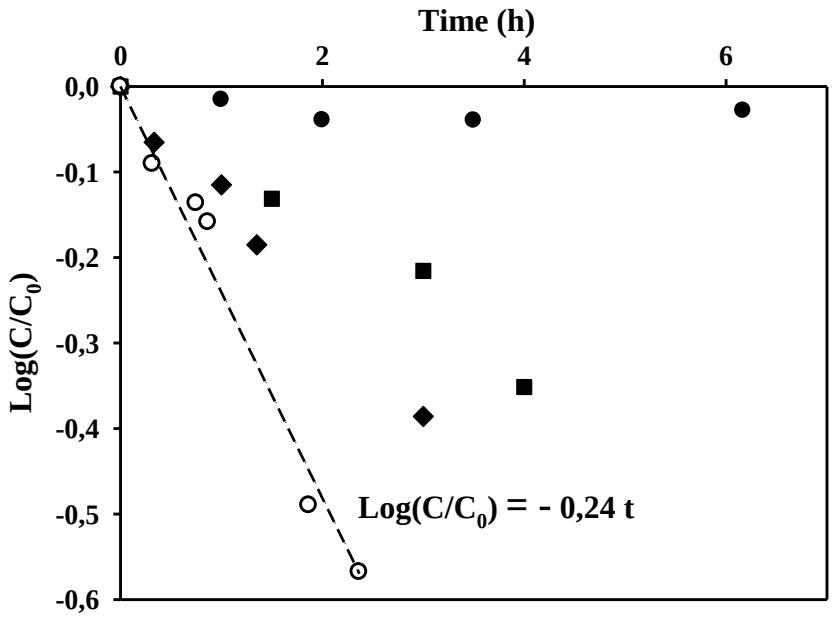

Figure 3

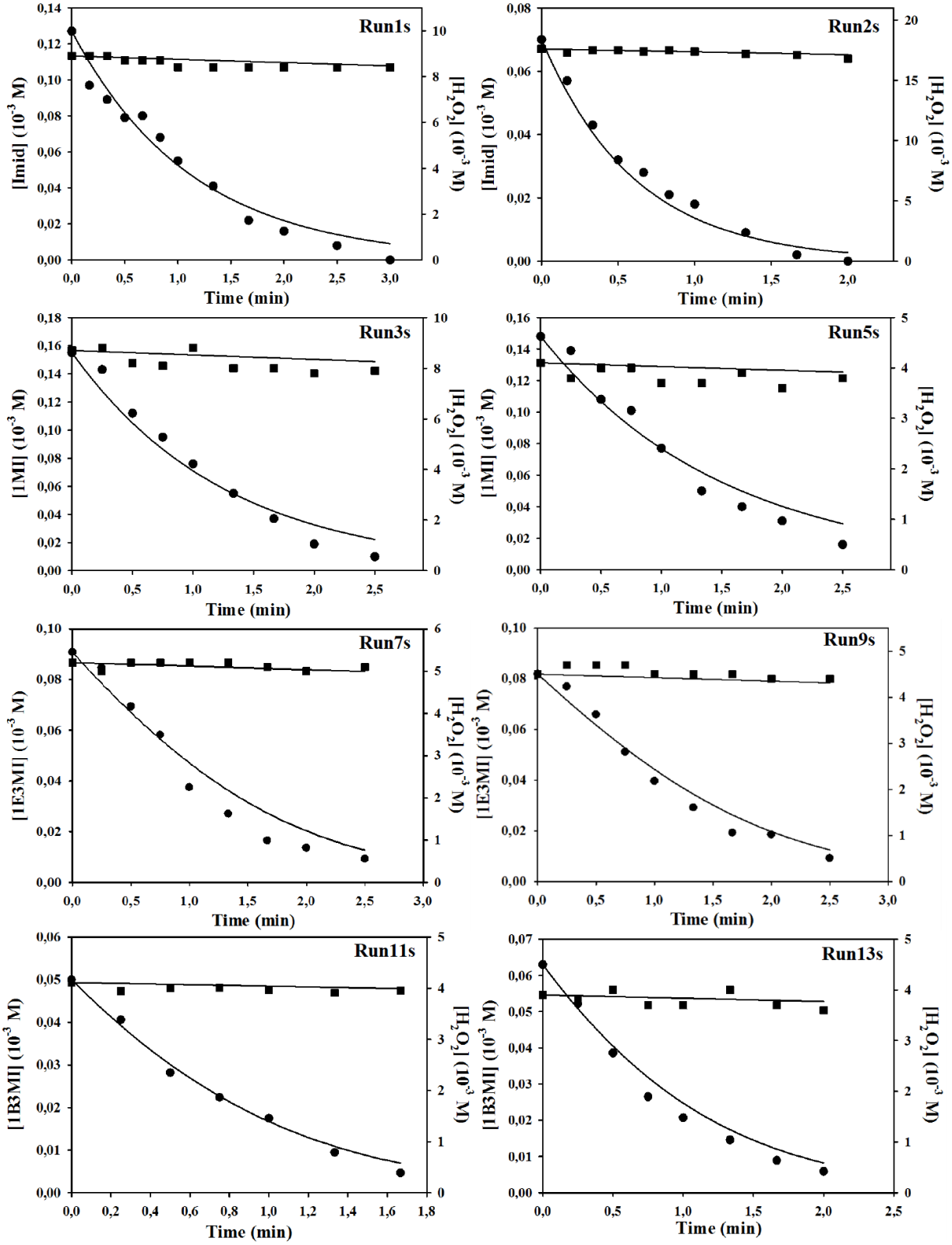
Run1s
[Imid] (10^{-3} M)
[H_2O_2] (10^{-3} M)
Time (min)
Run2s
[Imid] (10^{-3} M)
[H_2O_2] (10^{-3} M)
Time (min)
Run3s
[1MI] (10^{-3} M)
[H_2O_2] (10^{-3} M)
Time (min)
Run5s
[1MI] (10^{-3} M)
[H_2O_2] (10^{-3} M)
Time (min)
Run7s
[1E3MI] (10^{-3} M)
[H_2O_2] (10^{-3} M)
Time (min)
Run9s
[1E3MI] (10^{-3} M)
[H_2O_2] (10^{-3} M)
Time (min)
Run11s
[1B3MI] (10^{-3} M)
[H_2O_2] (10^{-3} M)
Time (min)
Run13s
[1B3MI] (10^{-3} M)
[H_2O_2] (10^{-3} M)
Time (min)

Figure 4

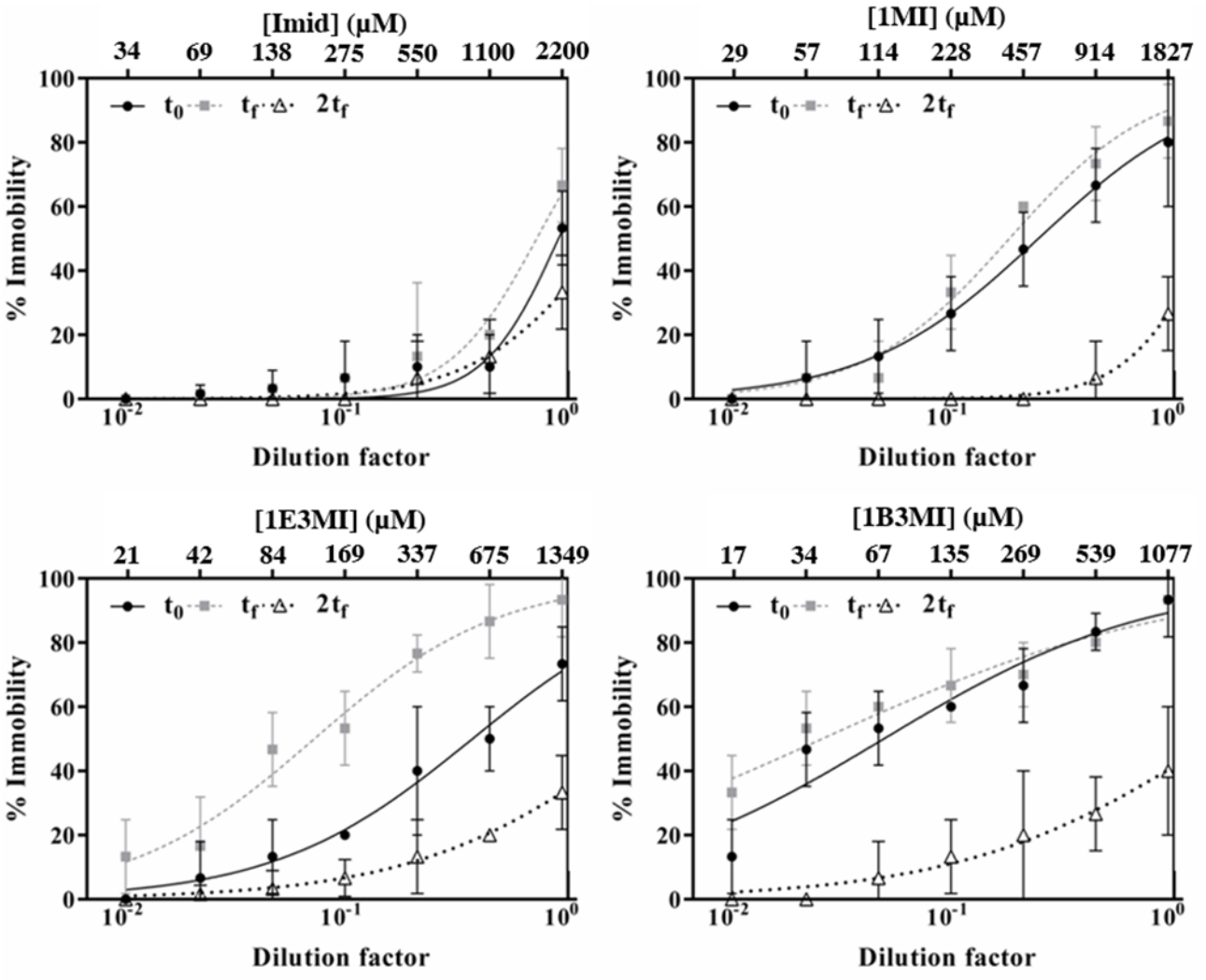
[Imid] (µM)
34 69 138 275 550 1100 2200
[1MI] (µM)
29 57 114 228 457 914 1827
[1E3MI] (µM)
21 42 84 169 337 675 1349
[1B3MI] (µM)
17 34 67 135 269 539 1077
t0 tf 2tf
% Immobility
Dilution factor
10-2 10-1 100

Figure 5

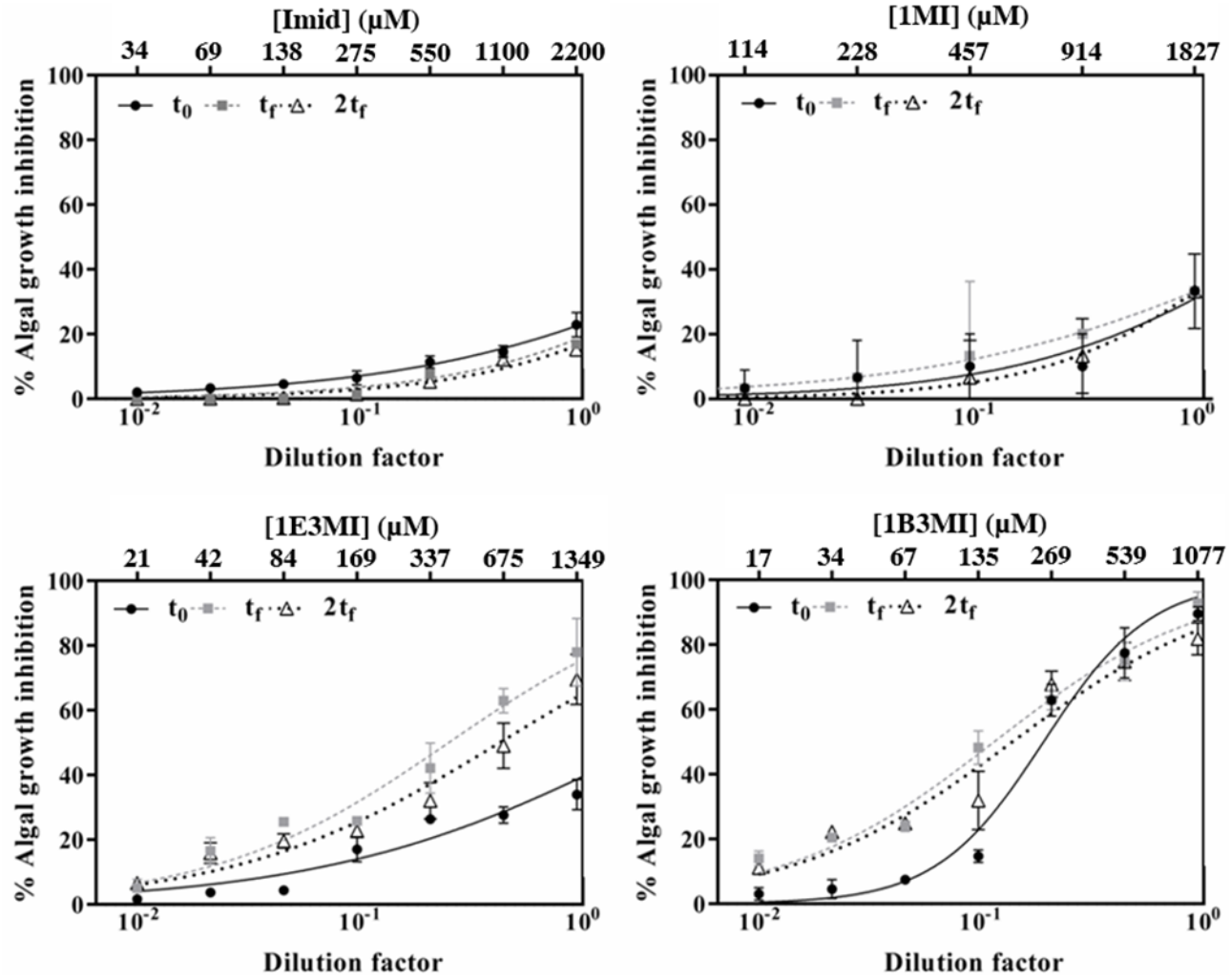
[Imid] (µM)
34 69 138 275 550 1100 2200
[1MI] (µM)
114 228 457 914 1827
[1E3MI] (µM)
21 42 84 169 337 675 1349
[1B3MI] (µM)
17 34 67 135 269 539 1077
% Algal growth inhibition
Dilution factor
t_0 t_f $2t_f$

Figure 6

Figure

Figure 1. Structural formulas of the investigated compounds.

Figure 2. Cylindrical batch photoreactor scheme.

Figure 3. Biodegradation test of the imidazole. ●: 1th recharge; ■: 4th recharge; ◆: 6th recharge; ○: 10th recharge. T = 25 °C. [VSS]= 3.0 g·l^{-1}.

Figure 4. Results of validation procedure. Predicted (continuous lines) and experimental (symbols) concentration-time profiles for S_i oxidation by means of the UV_{254}/H_2O_2 advanced oxidation process. (●) [S_i], (■) [H_2O_2]. T = 25 °C. The initial concentrations of the reagents and the initial pH of the solutions were reported in Table 5.

Figure 5. Dose-response curve describing the effects of Imid, 1MI, 1E3MI$^+$, 1B3MI$^+$ and its UV_{254}/H_2O_2 by-products on mobility of *D. magna*.

Figure 6. Dose-response curve describing the inhibitory effects of Imid, 1MI, 1E3MI$^+$, 1B3MI$^+$ and its UV_{254}/H_2O_2 by-products on growth of *R. subcapitata*.

Table 1. Imid, 1MI, 1E3MI, and 1B3MI molar absorption coefficient at 254 nm and pH=7.0.

Table 2. UV_{254}/H_2O_2 kinetic scheme along with the kinetic parameters.

Table 3. Initial conditions of the $UV_{254}/H_2O_2/S_i$ runs adopted during the optimization procedure and the calculated percentage standard deviations on the examined species.

Table 4. $k_{HO/Si}$ values estimated with both numerical and competition kinetic methods. *evaluated through the data of experimental UV_{254}/H_2O_2 runs in presence of benzoic acid ($[BA]_0 = [S_i]_0 = 1.5\cdot10^{-4}$ M) and $[H_2O_2]_0 = 6.5\cdot10^{-3}$ M. § Arouma et al., (1989). † Ching et al. (1993). ‡ Rao et al. (1975).

Table 5. Initial conditions of the $UV_{254}/H_2O_2/S_i$ runs used for validate the model and the calculated percentage standard deviations on the examined species.

Table 6. Normalized TOC and COD concentration at different reaction times.

Table 7. Ecotoxicity of Imid, 1MI, 1B3MI$^+$ and 1E3MI$^+$ to *R. subcapitata* and *D. magna*. [a] Hazard ranking: ***** practically harmless; ** harmful to aquatic organisms; *** toxic to aquatic organisms.